The cation-p box is a specific phosphatidylcholine membrane targeting motif

Authors: Jiongjia Cheng, R. Goldstein, A. Gershenson, B. Stec, Mary F. Roberts

Published in *Journal of Biological Chemistry*, vol. 288, no. 21, pp. 14863-14873, 2013

THE JOURNAL OF BIOLOGICAL CHEMISTRY VOL. 288, NO. 21, pp. 14863–14873, May 24, 2013

The Cation-π Box Is a Specific Phosphatidylcholine Membrane Targeting Motif*[S]

Received for publication, March 4, 2013, and in revised form, March 29, 2013 Published, JBC Papers in Press, April 10, 2013, DOI 10.1074/jbc.M113.466532

Jiongjia Cheng[‡], Rebecca Goldstein[§], Anne Gershenson[§], Boguslaw Stec[¶], and Mary F. Roberts[‡1]

From the [‡]Department of Chemistry, Boston College, Chestnut Hill, Massachusetts 02467, the [§]Department of Biochemistry and Molecular Biology, University of Massachusetts, Amherst, Massachusetts 01003, and the [¶]Sanford-Burnham Medical Research Institute, La Jolla, California 92037

Background: Specific interactions of peripheral membrane proteins with phosphatidylcholine (PC) are poorly characterized.
Results: *Staphylococcus aureus* phosphatidylinositol-specific phospholipase C has poor affinity for PC. Introduction of two tyrosines generates a specific PC binding site.
Conclusion: The PC choline cation interaction with amino acid π systems forms the PC-specific site.
Significance: Well defined choline cation-aromatic π interactions may be a general motif to anchor proteins to PC-rich bilayers.

Peripheral membrane proteins can be targeted to specific organelles or the plasma membrane by differential recognition of phospholipid headgroups. Although molecular determinants of specificity for several headgroups, including phosphatidylserine and phosphoinositides are well defined, specific recognition of the headgroup of the zwitterionic phosphatidylcholine (PC) is less well understood. In cytosolic proteins the cation-π box provides a suitable receptor for choline recognition and binding through the trimethylammonium moiety. In PC, this moiety might provide a sufficient handle to bind to peripheral proteins via a cation-π cage, where the π systems of two or more aromatic residues are within 4–5 Å of the quaternary amine. We prove this hypothesis by engineering the cation-π box into secreted phosphatidylinositol-specific phospholipase C from *Staphylococcus aureus*, which lacks specific PC recognition. The N254Y/H258Y variant selectively binds PC-enriched vesicles, and x-ray crystallography reveals N254Y/H258Y binds choline and dibutyroylphosphatidylcholine within the cation-π motif. Such simple PC recognition motifs could be engineered into a wide variety of secondary structures providing a generally applicable method for specific recognition of PC.

Cells are dynamic systems where spatially and temporally localized signaling facilitates responses to the local environment. Variations in lipid composition between different organelles and between organelles and the plasma membrane (1) provide spatial localization of peripheral membrane proteins that recognize specific lipids. For example, a number of proteins specifically recognize rare, anionic phosphoinositides with stereospecific recognition of the phosphoinositide headgroups (2, 3). For pleckstrin homology, PROPPIN β propellers, and other domains, stereospecificity often depends on a network of hydrogen bonds between the phosphoinositide headgroup and conserved basic residues (2–4). Similarly, proteins specific to the anionic phospholipid phosphatidylserine (PS)[2] may coordinate Ca^{2+} ions for PS binding using conserved loop motifs as observed in annexin V (5) or directly bind PS via C2 domains as in coagulation factor V (6) and lactadherin (7) where polar side chains allow specific recognition of PS. The affinity of the proteins for the membrane may be further modulated by insertion of hydrophobic and aromatic amino acids into the bilayer (5, 6, 8) and/or multivalent interactions (3) via domain repeats (9) or specificity for more than one type of lipid (9, 10).

Although there are numerous examples of specific binding to anionic lipids, less is known about specificity for zwitterionic lipids such as phosphatidylethanolamine (PE) and phosphatidylcholine (PC). Specific binding via a trimethylammonium moiety, such as that found in PC headgroups, has been observed in proteins that bind proline betaine and glycine betaine (11, 12) or choline (13, 14) as well as proteins that bind methylated lysine in histones (15–17) or methylated arginine (18). In these structures, the methylammonium is the center of a cation-π box with the faces of 2 to 4 aromatic residues located within 4–5 Å of the methylated amine allowing cation-π interactions with the aromatic residues. In search of the trimethylammonium binding motif, we have reviewed the Protein Data Bank database, and the only known structures containing PC with the choline held in a cation-π box are those for phosphatidylcholine transfer protein (supplemental Table S1 presents a list of crystal structures with choline and choline-related molecules bound). However, additional interactions with the acyl chains assist in PC binding by the transfer protein (19), and it is unclear

* This work was supported, in whole or in part, by National Institutes of Health Grant R01 GM60418 (to M. F. R.).
[S] This article contains supplemental Tables S1 and S2 and Figs. S1 and S2.
The atomic coordinates and structure factors (codes 4I9J and 4I8Y) have been deposited in the Protein Data Bank (http://wwpdb.org/).
[1] To whom correspondence may be addressed: Merkert Chemistry Department, Boston College, Chestnut Hill, MA. Tel.: 617-552-3616; Fax: 617-552-2705; E-mail: mary.roberts@bc.edu.

[2] The abbreviations used are: PS, phosphatidylserine; diC_4PC, 1,2-dibutyroyl-*sn*-glycero-3-phosphocholine; diC_7PC, 1,2-diheptanoyl-*sn*-glycero-3-phosphocholine; FCS, fluorescence correlation spectroscopy; PC, 1-palmitoyl-2-oleoylphosphatidylcholine; PE, 1,2-dioleoylphosphatidylethanolamine; PG, 1,2-dioleoyl-*sn*-glycero-3-phospho-(1′-rac-glycerol); PI, L-α-phosphatidylinositol; PI-PLC, phosphatidylinositol-specific phospholipase C; PMe, 1,2-dioleoylphosphatidylmethanol; SUV, small unilamellar vesicle; WT, wild-type recombinant *S. aureus* PI-PLC; X_{PC}, mole fraction PC; PDB, Protein Data Bank.

whether the π-cation interaction by itself would provide sufficient binding energy to transiently bind a protein to the membrane.

To test the hypothesis that such a cation-π box might allow specific, but transient binding to a PC-rich membrane, we have engineered such a box into *Staphylococcus aureus* phosphatidylinositol-specific phospholipase C (PI-PLC). *S. aureus* PI-PLC and the related PI-PLC from *Bacillus thuringiensis* are secreted virulence factors for extracellular bacteria that target glycosylphosphatidylinositol-anchored proteins in the PC-rich outer membrane of eukaryotic cells (20, 21). Although *B. thuringiensis* PI-PLC has a high affinity for PC vesicles (8), the similar PI-PLC from *S. aureus* has virtually no affinity for PC vesicles. High resolution field-cycling NMR experiments on *B. thuringiensis* identified a discrete binding site for PC that is consistent with Tyr residues forming a cation-π box or sandwich (22). However, this motif is not present in the *S. aureus* enzyme, which displays much weaker binding to PC-rich vesicles and virtually no binding to pure PC vesicles (23). Interestingly, unlike most other cation-π boxes, which are often made up of aromatic residues located on β strands and/or on loops with the separation required to sandwich a methyl ammonium between at least two π systems, the putative *B. thuringiensis* PI-PLC cation-π box is proposed to be located on adjacent α helices on the outside of a β-barrel. The addition of two tyrosine residues to the *S. aureus* PI-PLC introduces a specific binding site for PC that we characterize with several biophysical techniques including fluorescence correlation spectroscopy, high resolution field cycling NMR, as well x-ray crystallography. The molecular details of the engineered PC site in *S. aureus* PI-PLC suggest that it should be feasible to engineer similar PC headgroup-specific membrane binding modules into other proteins.

EXPERIMENTAL PROCEDURES

S. aureus PI-PLC Expression, Purification, Modification, and Enzymatic Activity—Recombinant *S. aureus* PI-PLC was produced and purified as described previously (24). The gene for the N254Y/H258Y mutant was constructed from the wild-type recombinant PI-PLC gene using QuikChange site-directed mutagenesis methodology (Stratagene) and primers purchased from Operon. The sequence of the mutated gene was confirmed by Genewiz. The purity of the PI-PLC enzymes was above 95% as monitored by SDS-PAGE; concentrations were measured by the absorption at 280 using extinction coefficients of $\epsilon_{280} = 60280\ \text{M}^{-1}\ \text{cm}^{-1}$ for WT and $\epsilon_{280} = 63260\ \text{M}^{-1}\ \text{cm}^{-1}$ for N254Y/H258Y calculated by the web-based ProtParam software. Protein was stored at 4 °C until used. Other *S. aureus* PI-PLC variants constructed and verified in the same fashion include N254Y, D213C, D213C/N254Y/H258Y, and Y211A/N254Y/H258Y/Y290A; H258Y was characterized previously (24).

The fluorescent dye Alexa Fluor 488 carboxylic acid, succinimidyl ester from Invitrogen was used to modify the N terminus of PI-PLC proteins for FCS studies. For the field cycling NMR experiments, both wild-type and N254Y/H258Y proteins with D213C were modified with the spin labeling reagent 2,2,5,5-tetramethyl-L-oxyl-3-methyl methanethiosulfonate, obtained from Toronto Research Chemicals. Excess dye or spin labeling reagents were removed with three Bio-Spin 6 columns.

PI-PLC cleavage of PI in small unilamellar vesicles (SUV), prepared by sonication, with varying mole fractions of PC, X_{PC}, was monitored by ^{31}P NMR using a Varian VNMRS 600 spectrometer as described previously (23, 24). Phospholipids were obtained from Avanti Polar Lipids, Inc., and used without further purification. Most enzymatic assays were carried out in 50 mM MES with 1 mM EDTA and 0.1 mg/ml of BSA, pH 6.5, using 0.2 to 8 μg/ml of the PI-PLC enzymes. Buffers used in assays at other pH values have been described previously (23). Assays for each X_{PC} were run in duplicate.

Vesicle Binding Measured by Fluorescence Correlation Spectroscopy (FCS)—The partitioning of both wild-type recombinant *S. aureus* PI-PLC and the N254Y/H258Y mutant was measured by FCS as described previously (22, 25). The fluorescence was monitored at 22 °C with samples placed in chambered coverglass wells (Lab-Tek, Nunc), containing 10 nM labeled *S. aureus* PI-PLC protein and 1 mg/ml of BSA in 300 μl of 50 mM MES, pH 6.5 (the same buffer as used for enzymatic assays). SUVs of the anionic phospholipid dioleoylphosphatidylglycerol (used as the substrate analog) with different mole fractions of 1-palmitoyl-2-oleoyl-PC were prepared by sonication. FCS data were analyzed as previously described (23, 26). The fitted diffusion coefficient of free, Alexa Fluor 488-labeled *S. aureus* PI-PLC (D_{free}) was 50 $\pm$ 2 $\mu\text{m}^2\ \text{s}^{-1}$; D_{bound}, determined using vesicles containing fluorescent labeled lipids, was in the range of 12–15 $\mu\text{m}^2\ \text{s}^{-1}$. K_d values for each X_{PC} were determined in duplicate using different protein and SUV preparations. Once the binding profiles were established for WT and N254Y/H258Y proteins, a quicker centrifugation assay (27) to separate vesicle bound and free protein, with quantification of free protein with the Bio-Rad DC protein assay, was used to compare the fraction of other related protein variants bound to 1 mM PG/PC (1:4) in 50 mM MES, pH 6.5, with 140 mM salt added.

PI-PLC Line Broadening of diC_7PC ^{31}P Resonance—diC_7PC (Avanti Polar Lipids, Inc.) was titrated into a solution of 3 mg/ml (0.085 mM) of PI-PLC in the same MES buffer with 1 mM EDTA. Protein-induced line broadening at 242.76 MHz was measured on a Varian VNMRS 600 spectrometer. For other bacterial PI-PLCs with significant PC affinity, the lipid linewidth increases dramatically around the critical micelle concentration (1.5 mM (10)), as protein-lipid micelle complexes form, then decreases as more diC_7PC is added to reach a limiting line width. Proteins with weakened affinity for PC have very little effect on the diC_7PC ^{31}P line width (28). Line widths at a given diC_7PC concentration were measured in duplicate samples.

Intrinsic Fluorescence of PI-PLC—Intrinsic fluorescence measurements of PI-PLC (0.2 μM) were carried out on a Fluorolog spectrometer (Horiba Jobin Yvon FL3–22). Samples were excited at 282 nm, and changes in the fluorescence intensity at the emission maximum, 337 nm, upon the addition of diC_7PC were expressed as $(I - I_0)/I_0$, where I_0 is the emission intensity of protein alone and I is the intensity in the presence of diC_7PC. A small amount of background signal from pure buffer solution or buffer with different concentrations of diC_7PC was sub-

tracted from the control and sample intensities. The dependence of $(I - I_0)/I_0$ on diC_7PC concentrations reflects protein binding affinity for that short chain lipid (10, 28).

High Resolution ^{31}P Field Cycling NMR Spectroscopy—High resolution ^{31}P field cycling NMR spin lattice (R_1) relaxation measurements, using a custom-built high resolution field cycling system on a Varian Unity^{plus} 500 spectrometer (29), were carried out with *S. aureus* PI-PLC spin-labeled at D213C. This position is comparable with D205C in *B. thuringiensis* PI-PLC, where a spin label had the largest effect on ^{31}P relaxation (22). The much larger dipole of the unpaired electron can relax ^{31}P fast-exchanging into and out of a discrete binding site and back into the bilayer. The field dependence of the increase in R_1 caused by the spin label for each lipid (ΔR_1) in a vesicle compared with the control, unlabeled protein, can be fit with the following expression: $\Delta R_1 = R_{P\text{-}e}(0)/(1 + \omega^2\tau_{P\text{-}e}{}^2) + c$. Here $R_{P\text{-}e}(0)$ is the maximum relaxation enhancement for that fraction of ligand bound to the spin-labeled protein, and $\tau_{P\text{-}e}$ is the correlation time for the bound phospholipid/spin-labeled PI-PLC interaction. A constant residual R_1 at higher fields, c, is likely to reflect a limiting chemical shift anisotropy contribution due to the paramagnetic interaction.

The parameters $R_{P\text{-}e}(0)$ and $\tau_{P\text{-}e}$ along with the total spin-labeled PI-PLC concentration, [PI-PLC-SL], and phospholipid concentration, L_o, are related to $r_{P\text{-}e}$, the distance between the phospholipid ^{31}P and the nitroxide when the ligand is bound (22). To a first approximation we assume that if there is a discrete site on the protein for an individual phosphorylated molecule, it is saturated with 5 mM of the ligand. We also assume that we are looking at a single PC or phosphatidylmethanol (PMe) binding in a given site for a time approaching 1–2 μs, long enough to suggest a specific complex as opposed to nonspecific lateral diffusion of the lipids around the protein, and that only phospholipid in the outer leaflet of the bilayer is in contact with the protein. For these small vesicles on average about 2/3 of the total of a specific phospholipid is in the outer monolayer. The average distance of the bound phospholipid on the protein at a specific site is calculated from the following expression.

$$r_{P\text{-}e}{}^6 = [\text{PI-PLC-SL}]/\{(2/3)[L]_o\} \times (S^2\tau_{P\text{-}e}/R_{P\text{-}e}(0))(0.3\ \mu^2(h/2\pi)^2\gamma_p{}^2\gamma_e{}^2) \quad \text{(Eq. 1)}$$

S^2, the order parameter of the electron spin-^{31}P dipolar interaction, is approximated as 1 because of the long $r_{P\text{-}e}$ compared with the size of local picosecond motions; μ, γ_P, and γ_e are well defined physical constants.

Crystallization and Structure Determination—S. aureus PI-PLC N254Y/H258Y was crystallized in three different conditions in 150 mM ammonium acetate, 100 mM sodium acetate, pH 4.6, and 100 mM magnesium nitrate with the following additives and treatments. (i) Crystals in the absence of choline compounds were grown with 26% PEG 4000; prior to crystallization, the protein was incubated with 100 mM *myo*-inositol for 2 h. (ii) Crystals with choline bound to the protein were grown with 26% PEG 4000; prior to crystallization, N254Y/H258Y was incubated with 30 mM glycerophosphocholine and 25 mM choline chloride. Before data collection, the crystals were soaked for 2 h in the crystallization buffer with the addition of 33% PEG 400 and 500 mM choline chloride. (iii) Crystals with diC_4PC bound to the protein were grown with 27% PEG 4000; protein was pretreated with glycerophosphocholine and choline chloride. Before data collection, the crystals were soaked in the crystallization buffer with 90 instead of 100 mM magnesium nitrate, 30% PEG 4000 and 100 mM diC_4PC (below its CMC ~250 mM (30)).

For all crystallizations, purified PI-PLC proteins were diluted to a concentration of 10 mg/ml and crystallized at 20 °C by vapor diffusion, using hanging drops of 3 μl. Single large crystals (0.5–0.7 mm) appeared overnight. Suitable crystals were mounted in nylon loops and frozen in liquid nitrogen. Data were collected at 100 K using an in-house Rigaku MicroMax-07 HF high-intensity microfocus rotating Cu anode x-ray generator, coupled with Osmic VariMax Optics and a R-Axis IV++ image plate area detector. Data were indexed and reduced using HKL2000 (31). All structures were solved by molecular replacement in PHENIX (32) using PHASER (33), with the previous H258Y structure (24) as a model. All models were refined in PHENIX with manual model building in COOT (34). Ligands and ligand restraints were generated using sketcher in CCP4 (35). Structural comparisons were made using SSM superposition (36) in COOT and alignment in PyMOL (Schrodinger). PROCHECK was used for structure validation (37).

RESULTS

Comparing B. thuringiensis and S. aureus PI-PLC—Bacterial PI-PLCs are single domain enzymes with active sites located at the center of a TIM-like barrel folding motif (24, 38, 39). PI-PLC from *B. thuringiensis* binds to PC-rich vesicles; residues located on the loop connecting helices F and G (notably Trp-242), as well several tyrosines located on helix G (Tyr-246, Tyr-247, Tyr-248, Tyr-251) were implicated in binding to PC interfaces (22, 28). Sequence and structural alignments of the *B. thuringiensis* and *S. aureus* PI-PLC enzymes show that whereas Tyr-246 and Tyr-248 in the *Bacillus* enzyme correspond to Tyr-253 and Tyr-255 in *S. aureus*, the other two tyrosine residues (247 and 251) in the *Bacillus* enzyme have been replaced with Asn-254 and His-258 in the *S. aureus* enzyme (Fig. 1*A*). *S. aureus* PI-PLC binds to PC-rich membranes with much lower affinity than does the *Bacillus* enzyme and has virtually no affinity for pure PC vesicles (23). This fact suggests that the higher affinity of the *Bacillus* enzyme for PC is associated with the presence of an aromatic box that creates a binding site for the choline. We hypothesized that mutating Asn-254 and His-258 to tyrosines (N254Y/H258Y) could introduce a specific PC binding site in *S. aureus* PI-PLC. This expectation was based on the observation that the site could utilize cation-π interactions to bind the PC headgroup.

Vesicle Binding and Enzymatic Activity of N254Y/H258Y S. aureus PI-PLC—FCS was used to measure binding of the WT and mutated enzymes to SUVs. We used low (~10 nM) enzyme concentrations similar to those used for enzymatic assays. WT, Y253S/Y255S, and N254Y/H258Y proteins were fluorescently labeled at the N terminus with a succinimidyl ester of Alexa Fluor 488, and apparent K_d values for PG/PC SUVs were measured as a function of the mole fraction PC, X_{PC} (Fig. 1*B*). All

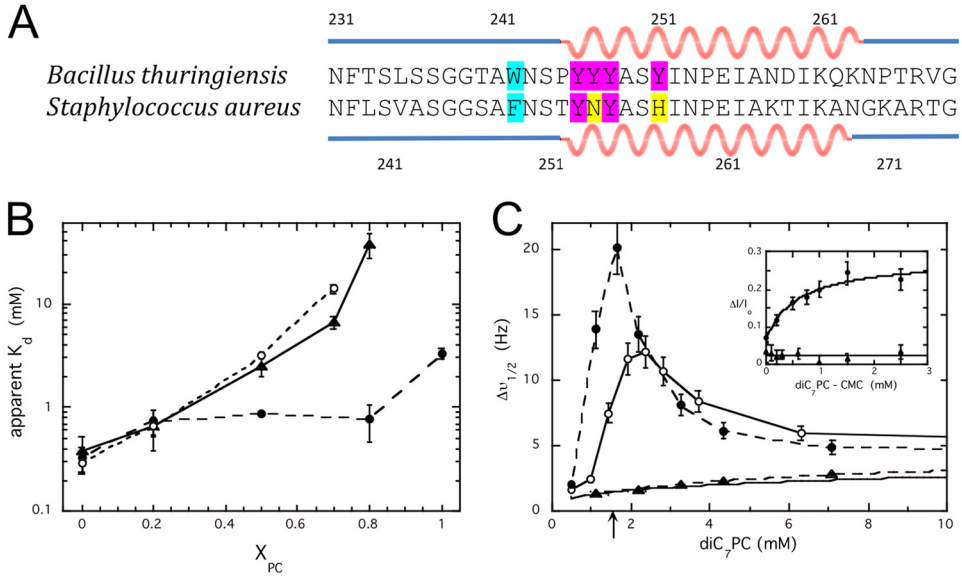

FIGURE 1. **Inserting the two missing Tyr residues generates PC specificity.** *A*, alignment of the F/G helix region of *B. thuringiensis* (PDB 1T6M) and *S. aureus* (PDB 3V18) PI-PLC. The secondary structure is shown *above* the alignment. Tyr residues are shaded *pink* and *S. aureus* Asn-254 and His-258 are shaded *yellow*. *B. thuringiensis* Trp-242 and *S. aureus* Phe-249 are shaded *blue*, these residues are important for membrane binding. *B*, apparent binding constants at pH 6.5 for *S. aureus* wild-type (▲), Y253S/Y255S (○), and N254Y/H258Y (●) partitioning to SUVs as a function of mole fraction PC (X_{PC}). *C*, ^{31}P linewidth of diC$_7$PC in the absence and presence (*dashed lines*) of 3 mg/ml of *S. aureus* PI-PLC variants: WT (▲) and N254Y/H258Y (●). The linewidth of diC$_7$PC without protein shows a small increase as micelles form (*solid line*). For comparison, the diC$_7$PC linewidth is shown in the presence of the same amount of *B. thuringiensis* PI-PLC (○). The *inset* shows the relative change in intrinsic fluorescence of *S. aureus* N254Y/H258Y (●) as a function of the amount of micellar diC$_7$PC added (estimated as [diC$_7$PC] ~1.5 mM, where 1.5 mM is the critical micelle concentration for pure diC$_7$PC at 25 °C). WT protein, which displays no change in fluorescence, is shown for comparison (▲). The *line* is a hyperbolic fit to the data.

three proteins have similar affinities for $X_{PC} \leq 0.2$ vesicles, but both WT and Y253S/Y255S have low affinities once $X_{PC} \geq 0.5$, whereas N254Y/H258Y still has a millimolar affinity for these PC-rich vesicles. As the PC content increases the difference in binding between the double mutant protein and WT is quite pronounced. N254Y/H258Y has a 50-fold lower apparent K_d than WT for $X_{PC} = 0.8$ vesicles. Although WT shows virtually no binding (<8% is bound with 55 mM PC) to pure PC SUVs, N254Y/H258Y binds with an apparent K_d of 3.3 ± 0.4 mM.

Moderate salt concentrations dramatically reduce *S. aureus* PI-PLC binding to vesicles (23), providing a simple assay to demonstrate whether PC is binding via one or both of the tyrosines that were introduced into the PI-PLC variant. Wild-type PI-PLC, N254Y, H258Y, and N254Y/H258Y (0.2 mg/ml) were each incubated with 1 mM PG/PC (0.2 mM/0.8 mM) SUVs in 50 mM MES, pH 7.5, with 140 mM salt, followed by centrifugation to separate free protein from vesicle bound protein. The total phospholipid concentration of 1 mM was chosen to be close to the K_d for N254Y/H258Y measured by FCS. Under these conditions, no WT or N254Y protein was bound to the vesicles; however, 12% of H258Y and 59% of N254Y/H258Y were bound to the vesicles. This suggests that a tyrosine at residue 258 is required, and that a tyrosine at 254 significantly increases PC binding in the H258Y background. This same binding assay carried out with 1 mM PG/PE (0.2 mM/0.8 mM) was used to examine if N254Y/H258Y exhibited a preference for PC compared with PE. When N254Y/H258Y was incubated with either the PC or PE containing SUVs, 68% of the protein was bound to the PG/PC SUVs, whereas only 36% of the protein was bound to the PG/PE SUVs. The interactions of the protein with PC appear significantly stronger than with PE.

Additionally, binding of *S. aureus* PI-PLC enzymes to PC micelles was explored by monitoring the ^{31}P line width of diC$_7$PC in the presence of the protein (Fig. 1*C*). *B. thuringiensis* PI-PLC induces formation of large protein-micelle complexes right around the critical micelle concentration, and mutations that weaken association with PC reduce this change in ^{31}P line width (28). *S. aureus* PI-PLC and the Y253S/Y255S variant had little or no effect on the diC$_7$PC line width, consistent with poor binding to a PC interface. However, *S. aureus* N254Y/H258Y mimicked the behavior of the *B. thuringiensis* PI-PLC with a large increase in linewidth at the critical micelle concentration. The intrinsic fluorescence associated with the presence of aromatic residues in N254Y/H258Y also increased with the addition of micellar diC$_7$PC; this effect was not observed with the *S. aureus* WT protein (Fig. 1*C*, *inset*).

Effect of the Added PC Site on Enzymatic Activity—The addition of two tyrosines to helix G in *S. aureus* PI-PLC has apparently created a site on *S. aureus* PI-PLC that can bind one or more PC molecules. The question arises whether this enhanced PC binding influences enzyme activity. *S. aureus* PI-PLC enzymatic activity toward PI in vesicles is sensitive to both pH and salt concentration (23, 24), and PC in the interface both alters the optimal pH for activity and ameliorates the salt sensitivity of the WT enzyme. These kinetic effects are not due to specific PC binding but rather result from competition between anion binding to a specific pocket in *S. aureus* PI-PLC and formation of a more active homodimer that occludes the anion binding site. Like WT, *S. aureus* PI-PLC N254Y/H258Y specific activity increases with increasing enzyme concentration indicating the active form is still a dimer. At pH 6.5 in the absence of salt, specific activity shows a large increase with PC content for both

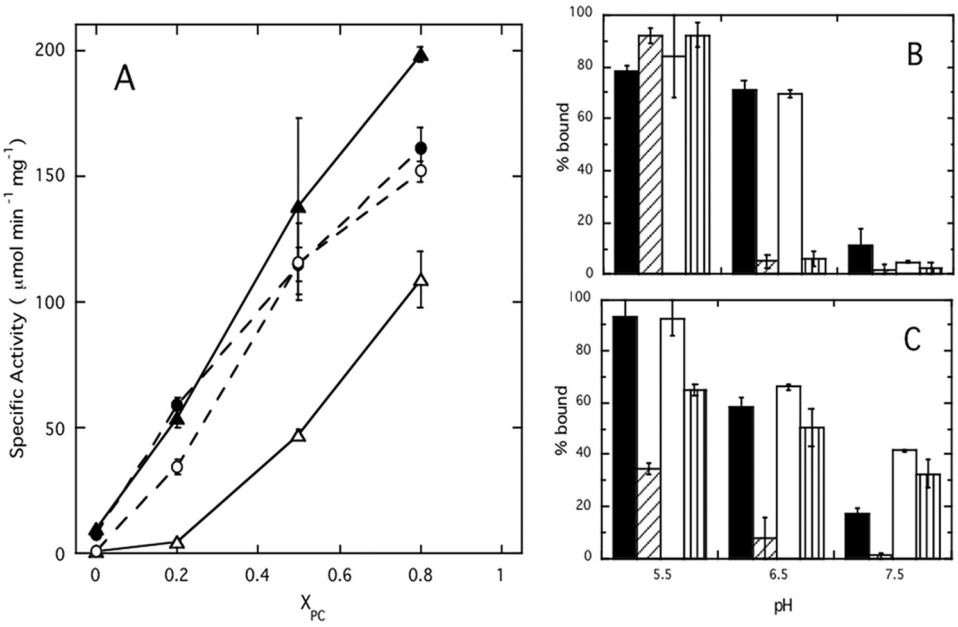

FIGURE 2. **In the presence of PC, N254Y/H258Y *S. aureus* PI-PLC is less salt-sensitive than wild-type.** *A,* specific activity of *S. aureus* WT (*triangles*) and N254Y/H258Y (*circles*) PI-PLC at pH 6.5 toward different vesicle compositions (X_{PC} = mole fraction PC) in the absence (*filled symbols*) and presence (*open symbols*) of 140 mM salt. The concentration of PI was kept at 4 mM with increasing amounts of PC. *B* and *C,* the apparent fraction of protein bound to (*B*) pure PG (6.2 mM) or (*C*) PG/PC (8.2:8.2 mM) SUVs (extracted from FCS data) is shown as a function of pH:WT in the absence (■) or presence (▨) of 140 mM salt; N254Y/H258Y in the absence (□) or presence (▥) of salt. *Error bars* represent the variation in parameters from experiments using different protein and SUV preparations.

N254Y/H258Y and WT (Fig. 2*A*). If salt is present neither WT nor N254Y/H258Y exhibits much activity toward pure PI SUVs, and salt reduces the activity of WT *S. aureus* PI-PLC even toward SUVs containing PC. However, once PC is present in the SUVs, the salt sensitivity of N254Y/H258Y enzyme is virtually abolished and the engineered enzyme exhibits activities in the presence of salt that are close to the values obtained without salt, whereas the activities of the WT are much lower in the presence of salt.

Specific activity toward PI in vesicles partially reflects how efficiently the protein partitions onto vesicles (24). For WT, the tightest binding is observed at pH 5.5, and added salt dramatically weakens binding to both pure PG and PG/PC (1:1) SUVs (Fig. 2, *B* and *C*). At pH > 5.5 in the absence of PC (Fig. 2*B*), the binding of both WT and N254Y/H258Y proteins are similarly inhibited by salt. However, once PC is present in the SUVs, N254Y/H258Y binding is not significantly affected by salt (Fig. 2*C*). The apparent K_d values for binding to $X_{PC} = 0.5$ SUVs, at pH 6.5 in the presence of 140 mM salt, were ~70 mM for WT and 2.6 ± 0.6 mM for N254Y/H258Y. Similarly, WT binding to pure PC SUVs was too low to measure, whereas N254Y/H258Y exhibited an apparent K_d of 5.4 ± 0.9 mM in the presence of salt (only about 50% higher than the apparent K_d in the absence of salt). Salt screens electrostatic interactions preventing WT *S. aureus* PI-PLC binding to these vesicles, but the engineered PC site in N254Y/H258Y allows binding to PC-containing interfaces even in the presence of salt.

Defining the PC Binding Site on a Molecular Level—Two experimental approaches were used to confirm the expectation that PC binds in direct proximity to the two introduced tyrosines (N254Y/H258Y): (i) high-resolution field cycling NMR analysis of the effect of spin-labeled protein on a mixed PC/PMe bilayer and (ii) x-ray crystallography structure determination for the N254Y/H258Y and H258Y *S. aureus* PI-PLC variants. Comparisons with the WT structure that has been described previously (24) offer insight not only into the conformational adaptability of the protein but also demonstrate that increased PC affinity results from PC binding mediated by the introduced tyrosine residues.

NMR Field Cycling Experiments with SUVs—Because the chemical shifts of different phospholipids are distinct, ^{31}P field cycling NMR is useful for identifying specific phospholipid interactions with a spin-labeled protein in multicomponent vesicles (22). In these experiments, differences in phospholipid ^{31}P relaxation rates provide a direct measure of the proximity of different phospholipid species to the spin label site. In particular, we have shown that for PC/PMe SUVs, *B. thuringiensis* PI-PLC spin labeled at D205C has a large effect on the ^{31}P relaxation rate of PC with a much smaller effect on PMe consistent with a PC site near the spin label and a bound PC lifetime between 1 μs and 1 ms. PMe, an anionic lipid that also competes with PI substrate, was used in these experiments, because over the course of 24 h there is some hydrolysis of PG by the enzyme and generation of diacylglycerol that causes vesicle fusion. *B. thuringiensis* Asp-205 aligns with *S. aureus* Asp-213, and spin labeling *S. aureus* PI-PLC at D213C has little effect on the PMe or PC resonances (Fig. 3*A*) under conditions (140 mM salt and 0.5 mg/ml of protein and 5 mM each phospholipid) where ~15–20% of this labeled WT protein is associated with the SUVs in the presence of salt. The field dependence data for D213C in the WT *S. aureus* PI-PLC background appears equivalent to what is seen for the SUVs in the absence of protein (22).

However, a very different profile is observed for spin-labeled D213C/N254Y/H258Y under the same conditions, and the

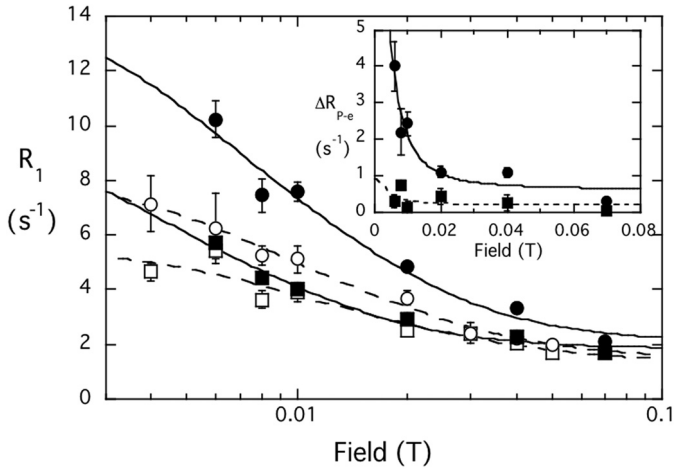

FIGURE 3. **The spin label at D213C perturbs lipid signals for the N254Y/H258Y mutant but not WT.** Effect of spin-labeled S. aureus PI-PLC (0.5 mg/ml) on PMe/PC (5:5 mM) SUVs:control PMe (□) and PC (○) mixed with spin-labeled D213C; PMe (■) and PC (●) with the spin-labeled D213C/N254Y/H258Y. The *inset* shows the difference in R_1 for each phospholipid ^{31}P specifically attributed to the spin label on D213C/N254Y/H258Y; the data are fit with $\tau_{P\text{-}e} = 2$ μs.

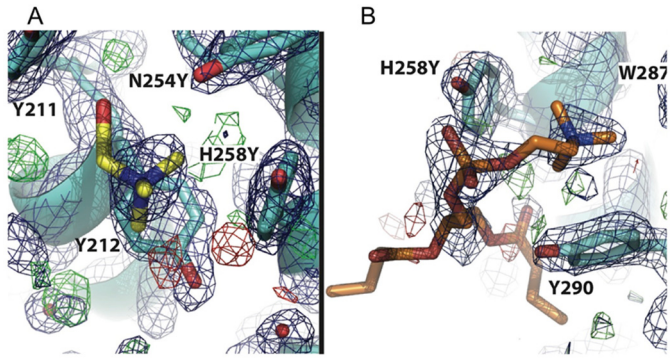

FIGURE 4. **Representative electron density for the choline binding site.** Electron density, in *dark blue* and contoured at 1σ, is shown with the model superimposed: *A*, binding site 1 with a choline molecule refined (PDB 4I9O); *B*, binding site 2 showing a molecule of diC$_4$PC fit to the electron density (PDB 4I9J). Residues that make up the binding pocket are indicated.

results for this variant resemble those for *B. thuringiensis* PI-PLC (Fig. 3). A potential complication to the average distance determination arises from the fact that *S. aureus* PI-PLC forms transient dimers on vesicle surfaces via helix B side chains (23). However, based on the dimer x-ray crystal structure, a spin label at residue 213 should be >35 Å from the active site of the opposing monomer, and 34–35 Å from H258Y on the opposing monomer. Because the distance dependence of the spin label falls off as $1/r^6$, the field cycling NMR should only report on an intramonomer PC site. The stronger effect exerted by the spin-labeled protein on the PC NMR relaxation rate compared with PMe therefore indicates that in the engineered protein (i) PC has a discrete binding site and (ii) it is near the region identified in the *B. thuringiensis* enzyme (22).

If we assume a single PC binds to the protein for the observed correlation time of the low field dispersion, then we can further use the ratio $\tau_{P\text{-}e}/\Delta R_{P\text{-}e}(0)$ to estimate a distance for each of these phospholipids to the spin label at residue 213. These parameters are obtained from fitting the relaxation as a function of field that is specifically due to the introduction of the spin label on N254Y/H258Y at D213C (Fig. 3, *inset*). The correlation time for the ^{31}P-electron dipolar interaction is 2 ± 1 μs and the extrapolated $\Delta R_{P\text{-}e}(0)$ values for the two phospholipids are 8.52 ± 1.28 s^{-1} (PC) and 0.71 ± 0.61 s^{-1} (PMe). Although $\tau_{P\text{-}e}$ is not known precisely, what is relevant in determining $r_{P\text{-}e}$ is the ratio $\tau_{P\text{-}e}/\Delta R_{P\text{-}e}(0)$, and this is very similar when fitting the data at 1 to 3 μs. For PC with $\tau_{P\text{-}e} = 2$ μs, this yields $r_{P\text{-}e}$ = 15.2 ± 0.4 Å. If the plot of ΔR_1 *versus* field is fit at 1- or 3-μs correlation times, there is at most a 0.5-Å variation in the estimated $r_{P\text{-}e}$. Interestingly, this value is a little longer than the $r_{P\text{-}e}$ extrapolated for the *B. thuringiensis* PI-PLC with a spin label attached at the same site (13.5 ± 0.2 Å (22)). The difference in $r_{P\text{-}e}$ for PC binding to the two PI-PLC proteins may look small, however, it is real because $\tau_{P\text{-}e}/\Delta R_{P\text{-}e}(0)$ (which differs by a factor of two for the two proteins) is proportional to $r_{P\text{-}e}{}^6$. There is a small effect on PMe, which should only occupy the active site with this amount of salt in the buffer (23). If one uses the fit with 2 μs $r_{P\text{-}e}$, bound PMe must be ~22–24 Å away, roughly about where the active would be from the spin label on residue 213. The key result is that the PC binding site we introduced in *S. aureus* N254Y/H258Y is located in the same area of the protein as it is in the *B. thuringiensis* PI-PLC.

Crystal Structures of N254Y/H258Y with Choline and DiC$_4$PC—To further explore the location of the introduced PC site, we obtained crystal structures of the N254Y/H258Y double mutant and compared it with those previously obtained for WT. The overall structure of the double mutant follows closely that of the native structure in basic conditions (24), with only slight deviations in the positioning of the mobile loop. The refined model of *S. aureus* PI-PLC N254Y/H258Y closely resembles that of the *Bacillus* enzyme especially in the region spanning the top halves of helices F and G. In this region, the structure of the N254Y/H258Y (PDB entry 4I8Y) differs only slightly from the basic form of the *S. aureus* native structure, aside from the mutations and the rotation of Tyr-212 and Tyr-255 by 83° and 22°, respectively. These rotamer differences are necessary to accommodate the larger side chains of the mutated residues. The rest of the structure shows only small variations associated with the inherent mobility of the enzyme and different amino acid content.

Initial crystallization trials to produce a crystal with a PC molecule bound to the N254Y/H258Y protein used solutions with 100 mM HEPES. Serendipitously, we found that rather than the PC, two HEPES molecules could be refined in the vicinity of the introduced tyrosines (supplemental Fig. S1 and Table S2). Because HEPES is cationic, the thought was that we might be able to get choline-containing molecules to bind if we soaked crystals with high enough concentrations of the potential ligands. Further evidence for the existence and the location of the binding site for a choline moiety was provided by crystal structures of N254Y/H258Y with choline and diC$_4$PC. These crystals were initially grown in 30 mM glycerol phosphocholine and 25 mM choline chloride. Under these conditions, no density was observed for either ligand in the vicinity of the new tyrosine residues. However, when these crystals were soaked for 2 h in a solution containing 500 mM choline or 100 mM diC$_4$PC, distinct density for these choline ligands was

TABLE 1
Crystallographic data for critical *S. aureus* PI-PLC crystals examined

Crystal	N254Y/H258Y	N254Y/H258Y + choline	N254Y/H258Y +diC$_4$PC
PDB ID	4I8Y	4I9O	4I9J
Diffraction data			
Resolution range (Å)	2.10–30.69Å	1.65–30.08	1.85–37.76
No. of reflections	18,210	36,554	24,758
Reflections in free set	933	1840	1279
Space group	$P2_12_12_1$	$P2_12_12_1$	$P2_12_12_1$
Unit cell			
a (Å)	85.55	85.98	85.65
b (Å)	57.78	57.58	57.47
c (Å)	61.38	61.69	61.75
Completeness	99.2%	97.2%	92.5
R_{merge}	9.9	5.8	8.4
Protein molecules in A.U.	1	1	1
Refinement			
R_{cryst} [a]	0.1781	0.1772	0.1627
R_{free} [b]	0.2312	0.2136	0.2076
No. residues	303	301	301
No. non-hydrogen protein atoms	2441	2449	2465
No. H_2O molecules	138	195	239
No. acetate molecules	1	2	1
No. chloride ions	1	1	0
Root mean square bonds (Å)	0.009	0.007	0.019
Root mean square deviation angles (°)	1.11	1.05	1.94
Ramachandran plot (%)			
Most favored	98.02	98.69	98.70
Additionally allowed	1.98	1.31	1.30
Generously allowed	0	0	0
Disallowed	0	0	0
Average *B*-factor (Å^2)	33.74	29.40	28.998

[a] $R_{cryst} = \{\Sigma\ (||F_o| - |F_c||)/|F_o|\}$, where $|F_o|$ and $|F_c|$ are the observed and calculated structure factor amplitudes, respectively.
[b] Brunger (1992).

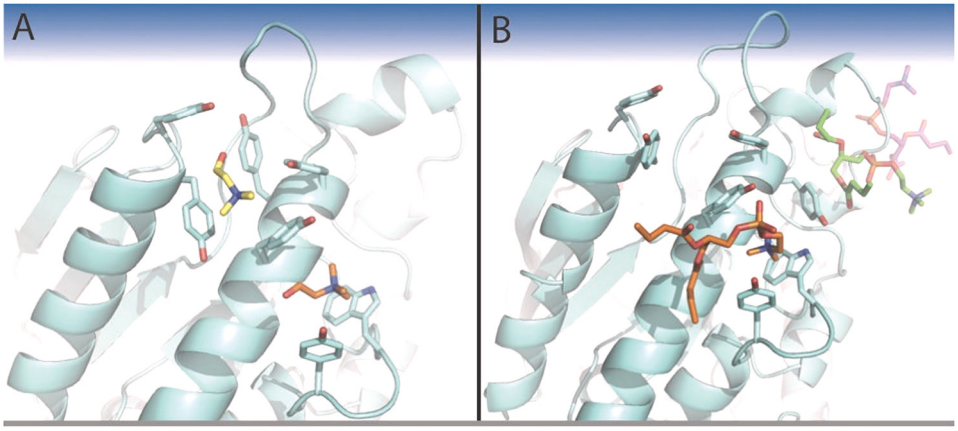

FIGURE 5. **Cationic ligand binding pockets on *S. aureus* PI-PLC N254Y/H258Y.** View of the two choline binding pockets (*A*) occupied by choline shown in *yellow* in site 1 and *orange* in site 2 (PDB entry 4I9O) or (*B*) diC$_4$PC (PDB entry 4I9J) with the lipid in choline site 2 in *orange*, diC$_4$PC below helix B in *green*, and diC$_4$PC associated with the anion binding pocket in *magenta*.

observed (representative density with the models superimposed is shown in Fig. 4). Statistics for the different crystal structures are presented in Table 1.

In the N254Y/H258Y structure with choline (PDB entry 4I9O), two molecules of that ligand could be identified (Fig. 5*A*). The quaternary amines of each choline were observed to bind on either side of H258Y, with the quaternary amine of choline 1 making cation-π interactions with the aromatic side chains of H258Y and Tyr-212, whereas choline 2 makes similar cation-π interactions with Trp-287 and Tyr-290. Comparison with an unliganded structure of N254Y/H258Y shows that the side chains of Tyr-211 and H258Y are rotated 77° and 100°, respectively (Fig. 6*A*). The rotation of Tyr-211 creates binding pocket 1, whereas the rotation of H258Y forms the right side of binding pocket 1, as well as the left side of binding pocket 2.

The structure for the mutant protein in the presence of the short-chain lipid diC$_4$PC (PDB entry 4I9J) showed three molecules of diC$_4$PC bound (Fig. 5*B*). One molecule of diC$_4$PC (refined with 80% occupancy) was located in choline binding pocket 2. The quaternary amines of the choline and diC$_4$PC ligands are completely superimposable. The phosphate moiety of diC$_4$PC makes additional polar contacts to the side chain hydroxyls of Tyr-290 and Tyr-258. Density for this ligand (Fig. 4*B*) is quite strong for the phosphocholine portion of the molecule and the glycerol moiety. However, there is substantial disorder at the lipid chains. No diC$_4$PC lipids were seen occupying choline binding site 1. However, the high concentration of lipid led to the observation of two additional diC$_4$PC molecules in the structure at sites not occupied by choline. One diC$_4$PC, found at 70% occupancy, was bound through polar

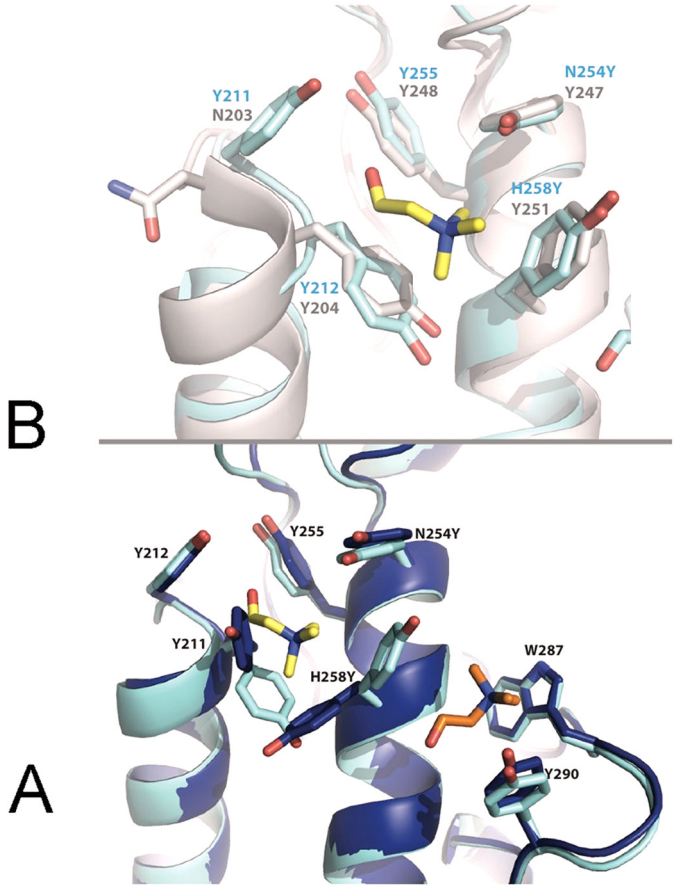

FIGURE 6. *A*, overlay of the *S. aureus* PI-PLC N254Y/H258Y structure without choline (*dark blue*, PDB entry 4I8Y) and with choline bound (*teal*, PDB entry 4I9O) showing that choline site 2 is preformed, whereas site 1 requires rotamer changes in side chains. *B*, overlay of choline site 1 in *S. aureus* N254Y/H258Y (*teal*) with the (*gray*) *B. thuringensis* PI-PLC (PDB entry 1T6M). Residues interacting with the cholines are identified.

contacts of the phosphate to the backbone carbonyls of Leu-37 and Lys-38 and the side chain hydroxyl of Ser-43 (supplemental Fig. S2*A*). An additional molecule of diC_4PC (80% occupancy) was observed (supplemental Fig. S2*B*) with the phosphate occupying an anion binding pocket (23, 24). Under the conditions this crystal was formed, an acetate ion would be a typical occupant of the anion pocket. The high levels of diC_4PC in the soaking liquor could easily outcompete the acetate ion. The observation of a diC_4PC phosphate interacting at the anion binding pocket is consistent with the proposal that anionic phospholipids (including substrate PI) in a vesicle can bind in this region (23), and are likely to be displaced when the surface concentration of the anionic lipid decreases. These two additional lipids are held by polar contacts that are not specific to choline or phosphatidylcholine.

Do Both Choline Sites in N254Y/H258Y Bind PC?—A comparison of *S. aureus* N254Y/H258Y PI-PLC structures in the absence or presence of a trimethylammonium ligands provides insights into the nature of the specific choline and PC sites. To accommodate the cationic ligand there are clear rotations of side chains in choline binding site 1, relative to the unliganded enzyme (Fig. 6*A*). Interestingly, in the choline bound conformation, binding pocket 1 of the double mutant overlays well with the side chains of the *B. thuringiensis* PI-PLC structure (PDB entry 1T6M) (Fig. 6*B*), whereas choline site 2 appears unique to the *S. aureus* PI-PLC mutant but resembles other choline binding sites that can use a Trp residue to form part of the cation-π box (supplemental Table S1). Although the secondary structure of the two proteins is quite different, the spatial arrangement of tyrosine residues in choline site 1 is very similar to how choline is bound in OpuBC (14). However, we only see soluble diC_4PC binding in choline site 2 and not in choline site 1. This could be the result of weak PC binding, at least in the absence of a bilayer (which could locally increase the choline headgroup concentration so that binding occurs more readily), or it could be attributed to the difficulty in moving side chains in site 1 to accommodate a choline moiety, which might be more difficult when the choline is part of a phospholipid molecule.

The field cycling ^{31}P NMR experiments provide insight into where PC presented in a bilayer binds on the protein, for at least 2 μs (22). For the same amount of protein and phospholipids, $\tau_{P\text{-}e}/\Delta R_{P\text{-}e}(0)$, which is proportional to $r_{P\text{-}e}{}^6$, is 2.35×10^{-7} s^2 for N254Y/H258Y, and 1.48×10^{-7} s^2 for *B. thuringiensis* PI-PLC, consistent with PC binding closer to the spin label site in *B. thuringiensis* PI-PLC than in the engineered *S. aureus* protein. The *Bacillus* protein only has choline site 1 available for PC binding. Furthermore, if a PC molecule occupied *both* choline sites when N254Y/H258Y was bound to PC/PMe SUVs, there should be a considerably stronger relaxation of the ^{31}P nucleus that is roughly twice as effective as when a single PC binds to the protein. Because $\tau_{P\text{-}e}/\Delta R_{P\text{-}e}(0)$ is larger for the *S. aureus* N254Y/H258Y, only one PC binds well with a $\geq$2 μs lifetime. In turn, the observation that the averaged distance of the spin label to the bound PC ^{31}P is larger in N254Y/H258Y than in *B. thuringiensis* PI-PLC is consistent with PC binding to the *S. aureus* protein in choline site 2. Energy minimization of the crystal structure placed the isolated chains of diC_4PC against the protein, but the same orientation of the choline moiety could easily be occupied with a longer chain phospholipid anchored in a bilayer (Fig. 7*A*).

As further evidence for occupation of a single PC site in N254Y/H258Y, we generated Y211A/N254Y/H258Y/Y290A. Mutation of Tyr-290 to alanine should abolish choline affinity for site 2. Tyr-211 is not conserved in *B. thuringiensis* PI-PLC and must rotate by 77° to accommodate the choline cation. Its removal might be expected to enhance PC binding, if site 1 is significantly populated by a PC molecule. Using the centrifugation assay for partitioning of Y211A/N254Y/H258Y/Y290A onto PG/PC (0.2 mM/0.8 mM) SUVs, we found little protein associated with the SUVs with 1 mM total phospholipid. With 8 mM total phospholipid 7.7 $\pm$ 3.8% of the protein was bound. In essence, abolishing choline site 2 prevents *S. aureus* N254Y/H258Y from binding to PC-containing SUVs. This confirms that although two choline sites were introduced into *S. aureus* N254Y/H258Y, only preformed site 2 interacts significantly with a PC headgroup.

DISCUSSION

Sandwiches, cages, or boxes composed of aromatic amino acid π systems of aromatic amino acids are a facile way to bind trimethylammonium moieties via cation-π interactions. In so doing they provide a specific recognition motif for the head-

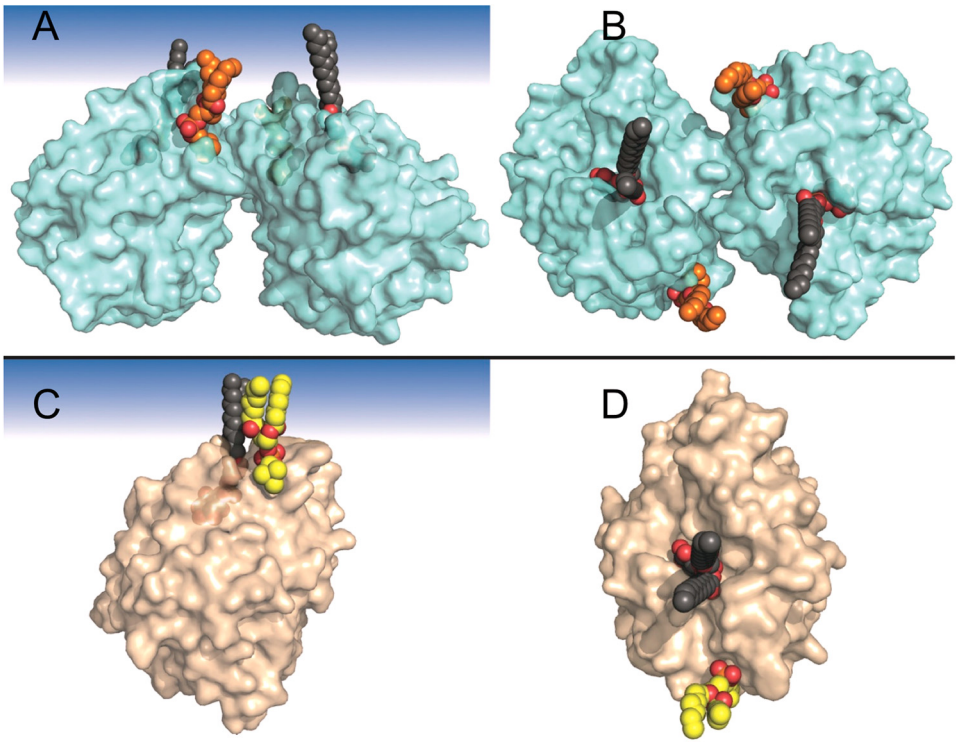

FIGURE 7. ***In silico* models of PC and PI binding to discrete sites on *S. aureus* PI-PLC N254Y/H258Y and *B. thuringiensis* PI-PLC.** The *S. aureus* mutant structure is shown as a dimer (mediated through helix B) with one molecules of diC_7PC in site 2 (*orange*) and one molecule of PI (*dark gray*) in the active site in views (*A*) with the membrane interface at the *top*, and (*B*) looking down from the membrane. The *B. thuringiensis* monomer is shown with diC_7PC modeled in site 1 (*yellow*) along with one molecule of PI (*dark gray*) in the active site in views (*C*) with the membrane at the top or (*D*) looking down from the membrane.

groups of zwitterioinic phospholipids. *Bacillus* PI-PLC is activated by PC (10), in large part by enhancing vesicle binding (25). The G helix region of *Bacillus* PI-PLCs has several Tyr residues that could form a sandwich or cage around a choline group (22, 28), but how and whether PC binds to this box was unclear. Attempts to transplant this box into *S. aureus* PI-PLC by introducing two "missing" tyrosine side chains in helix G generated catalytically active protein that binds much more tightly to PC-rich interfaces. Field cycling NMR suggest there are similarities in the position of PC bound to *B. thuringiensis* PI-PLC and to *S. aureus* N254Y/H258Y protein when the protein is transiently anchored on a vesicle. Although x-ray crystallography reveals two spatially close choline binding sites on the engineered protein (site 1 between tyrosines on helix F and helix G and site 2 between helix G and a loop), only choline site 2 between helix G and a loop is occupied by a PC molecule in the *S. aureus* protein. *B. thuringiensis* PI-PLC does not have the key tryptophan residue needed for choline site 2. However, all the side chains are correctly oriented for binding a choline (or PC) in what is analogous to *S. aureus* N254Y/H258Y site 1.

Although the specific cation-π PC binding site in *B. thuringiensis* PI-PLC (equivalent of choline site 1) and that in *S. aureus* PI-PLC (choline site 2) are different, the energetic contribution of these aromatic π-choline cation interactions to PC binding should be similar and different from values for partitioning a tyrosine side chain into a bilayer (40). We can use the apparent K_d values as a way to assess this. The relative change in vesicle binding affinity when the cation-π site is abolished, K_d(no PC site)/K_d(intact PC site), should be similar for both enzymes. Data for $X_{PC} = 0.8$ SUVs were chosen for the comparison, because no K_d could be obtained for *S. aureus* WT binding to pure PC SUVs (23). For the *S. aureus* PI-PLC, K_d(WT)/K_d(N254Y/H258Y) = 48. For *B. thuringiensis* PI-PLC, the Y251A mutant was selected as one where the site analogous to choline site 1 should be abolished (Tyr-251 is the equivalent of *S. aureus* H258Y). Binding data at the same mole fraction PC (41) yield K_d(Y251A)/K_d(WT) = 45. Thus, the absence of a PC site, whether it is analogous to choline site 1 or choline site 2 in the *S. aureus* mutant, has essentially equivalent effects on vesicle binding. This translates to a change in free energy (at 22 °C, the temperature of the FCS experiments) of 9.5 and 9.3 kJ/mol for losing this cation-π interaction. For comparison, partitioning of a tyrosine or a tryptophan side chain from the interior of a bilayer to water is estimated as 3.9 or 7.7 kJ/mol, respectively (40). Clearly, cation-π interactions between proteins and the PC headgroup can stabilize the transient membrane binding needed for peripheral proteins. Invoking these interactions provides an explanation for why *S. aureus* PI-PLC N254Y/H258Y binds to pure PC bilayers with significantly weaker affinity than *B. thuringiensis* PI-PLC. Tallying up the tyrosine residues around the rim of the $\alpha\beta$-barrel it is clear that the *B. thuringiensis* PI-PLC has far more aromatic residues that could either (i) insert into the bilayer or (ii) form transient cation-π complexes.

These results, combined with structural studies of proteins that bind methyl-Lys, methyl-Arg, or choline using similar cation-π cages/boxes suggest that this cation-π motif has evolved in a variety of secondary structural contexts ranging from β barrels to β propellers to α helices and loops, anywhere that aromatic side chains can be separated by 8–10 Å to allow space

for binding a methylammonium moiety. In the case of membranes, such π system motifs could provide a general way to introduce specific yet transient interactions of peripheral membrane proteins with PC headgroups.

Acknowledgment—We thank Prof. Alfred G. Redfield for access to his high-resolution field cycling device and for sealing samples.

REFERENCES

1. van Meer, G., Voelker, D. R., and Feigenson, G. W. (2008) Membrane lipids. Where they are and how they behave. *Nat. Rev. Mol. Cell Biol.* **9,** 112–124
2. Lemmon, M. A. (2008) Membrane recognition by phospholipid-binding domains. *Nat. Rev. Mol. Cell Biol.* **9,** 99–111
3. Kutateladze, T. G. (2010) Translation of the phosphoinositide code by PI effectors. *Nat. Chem. Biol.* **6,** 507–513
4. Krick, R., Busse, R. A., Scacioc, A., Stephan, M., Janshoff, A., Thumm, M., and Kühnel, K. (2012) Structural and functional characterization of the two phosphoinositide binding sites of PROPPINs, a β-propeller protein family. *Proc. Natl. Acad. Sci. U.S.A.* **109,** E2042–E2049
5. Concha, N. O., Head, J. F., Kaetzel, M. A., Dedman, J. R., and Seaton, B. A. (1993) Rat annexin V crystal structure. Ca^{2+}-induced conformational changes. *Science* **261,** 1321–1324
6. Macedo-Ribeiro, S., Bode, W., Huber, R., Quinn-Allen, M. A., Kim, S. W., Ortel, T. L., Bourenkov, G. P., Bartunik, H. D., Stubbs, M. T., Kane, W. H., and Fuentes-Prior, P. (1999) Crystal structures of the membrane-binding C2 domain of human coagulation factor V. *Nature* **402,** 434–439
7. Shao, C., Novakovic, V. A., Head, J. F., Seaton, B. A., and Gilbert, G. E. (2008) Crystal structure of lactadherin C2 domain at 1.7-Å resolution with mutational and computational analyses of its membrane binding motif. *J. Biol. Chem.* **283,** 7230–7241
8. Feng, J., Wehbi, H., and Roberts, M. F. (2002) Role of tryptophan residues in interfacial binding of phosphatidylinositol-specific phospholipase C. *J. Biol. Chem.* **277,** 19867–19875
9. Knight, J. D., Lerner, M. G., Marcano-Velázquez, J. G., Pastor, R. W., and Falke, J. J. (2010) Single molecule diffusion of membrane-bound proteins. Window into lipid contacts and bilayer dynamics. *Biophys. J.* **99,** 2879–2887
10. Zhou, C., Qian, X., and Roberts, M. F. (1997) Allosteric activation of phosphatidylinositol-specific phospholipase C. Specific phospholipid binding anchors the enzyme to the interface. *Biochemistry* **36,** 10089–10097
11. Schiefner, A., Breed, J., Bösser, L., Kneip, S., Gade, J., Holtmann, G., Diederichs, K., Welte, W., and Bremer, E. (2004) Cation-π interactions as determinants for binding of the compatible solutes glycine betaine and proline betaine by the periplasmic ligand-binding protein ProX from *Escherichia coli*. *J. Biol. Chem.* **279,** 5588–5596
12. Tschapek, B., Pittelkow, M., Sohn-Bösser, L., Holtmann, G., Smits, S. H., Gohlke, H., Bremer, E., and Schmitt, L. (2011) Arg149 is involved in switching the low affinity, open state of the binding protein AfProX into its high affinity, closed state. *J. Mol. Biol.* **411,** 36–52
13. Oswald, C., Smits, S. H., Höing, M., Sohn-Bösser, L., Dupont, L., Le Rudulier, D., Schmitt, L., and Bremer, E. (2008) Crystal structures of the choline/acetylcholine substrate-binding protein ChoX from *Sinorhizobium meliloti* in the liganded and unliganded-closed states. *J. Biol. Chem.* **283,** 32848–32859
14. Pittelkow, M., Tschapek, B., Smits, S. H., Schmitt, L., and Bremer, E. (2011) The crystal structure of the substrate-binding protein OpuBC from *Bacillus subtilis* in complex with choline. *J. Mol. Biol.* **411,** 53–67
15. Nielsen, P. R., Nietlispach, D., Mott, H. R., Callaghan, J., Bannister, A., Kouzarides, T., Murzin, A. G., Murzina, N. V., and Laue, E. D. (2002) Structure of the HP1 chromodomain bound to histone H3 methylated at lysine 9. *Nature* **416,** 103–107
16. Jacobs, S. A., and Khorasanizadeh, S. (2002) Structure of HP1 chromodomain bound to a lysine 9-methylated histone H3 tail. *Science* **295,** 2080–2083
17. Collins, R. E., Northrop, J. P., Horton, J. R., Lee, D. Y., Zhang, X., Stallcup, M. R., and Cheng, X. (2008) The ankyrin repeats of G9a and GLP histone methyltransferases are mono- and dimethyllysine binding modules. *Nat. Struct. Mol. Biol.* **15,** 245–250
18. Tripsianes, K., Madl, T., Machyna, M., Fessas, D., Englbrecht, C., Fischer, U., Neugebauer, K. M., and Sattler, M. (2011) Structural basis for dimethylarginine recognition by the Tudor domains of human SMN and SPF30 proteins. *Nat. Struct. Mol. Biol.* **18,** 1414–1420
19. Roderick, S. L., Chan, W. W., Agate, D. S., Olsen, L. R., Vetting, M. W., Rajashankar, K. R., and Cohen, D. E. (2002) Structure of human phosphatidylcholine transfer protein in complex with its ligand. *Nat. Struct. Biol.* **9,** 507–511
20. Lovgren, A., Carlson, C. R., Eskils, K., and Kolsto, A. B. (1998) Localization of putative virulence genes on a physical map of the *Bacillus thuringiensis subsp. gelechiae* chromosome. *Curr. Microbiol.* **37,** 245–250
21. Daugherty, S., and Low, M. G. (1993) Cloning, expression, and mutagenesis of phosphatidylinositol-specific phospholipase C from *Staphylococcus aureus*. A potential staphylococcal virulence factor. *Infect. Immun.* **61,** 5078–5089
22. Pu, M., Orr, A., Redfield, A. G., and Roberts, M. F. (2010) Defining specific lipid binding sites for a peripheral membrane protein *in situ* using subtesla field cycling NMR. *J. Biol. Chem.* **285,** 26916–26922
23. Cheng, J., Goldstein, R., Stec, B., Gershenson, A., and Roberts, M. F. (2012) Competition between anion binding and dimerization modulates *S. aureus* phosphatidylinositol-specific phospholipase C enzymatic activity. *J. Biol. Chem.* **287,** 40317–40327
24. Goldstein, R., Cheng, J., Stec, B., and Roberts, M. F. (2012) Structure of the *S. aureus* PI-specific phospholipase C reveals modulation of active site access by a titratable π-cation latched loop. *Biochemistry* **51,** 2579–2587
25. Pu, M., Roberts, M. F., and Gershenson, A. (2009) Fluorescence correlation spectroscopy of phosphatidylinositol-specific phospholipase C monitors the interplay of substrate and activator lipid binding. *Biochemistry* **48,** 6835–6845
26. Cheng, J., Karri, S., Grauffel, C., Wang, F., Reuter, N., Roberts, M. F., Wintrode, P. L., and Gershenson, A. (2013) Does changing the predicted dynamics of a phospholipase C alter activity and membrane binding? *Biophys. J.* **104,** 185–195
27. Wehbi, H., Feng, J., Kolbeck, J., Ananthanarayanan, B., Cho, W., and Roberts, M. F. (2003) Investigating the interfacial binding of bacterial phosphatidylinositol-specific phospholipase C. *Biochemistry* **42,** 9374–9382
28. Shi, X., Shao, C., Zhang, X., Zambonelli, C., Redfield, A. G., Head, J. F., Seaton, B. A., and Roberts, M. F. (2009) Modulation of *Bacillus thuringiensis* phosphatidylinositol-specific phospholipase C activity by mutations in the putative dimerization interface. *J. Biol. Chem.* **284,** 15607–15618
29. Redfield, A. G. (2012) High-resolution NMR field cycling device for full range relaxation and structural studies of biopolymers on a shared commercial instrument. *J. Biomol. NMR* **52,** 159–177
30. Bian, J., and Roberts, M. F. (1992) Thermodynamic comparison of lyso- and diacylphosphatidylcholines. *J. Colloid. Interface Sci.* **153,** 420–428
31. Otwinowski, Z., and Minor, W. (1997) Processing of x-ray diffraction data collected in oscillation mode. *Methods Enzymol.* **276,** 307–326
32. Adams, P. D., Afonine, P. V., Bunkóczi, G., Chen, V. B., Davis, I. W., Echols, N., Headd, J. J., Hung, L. W., Kapral, G. J., Grosse-Kunstleve, R. W., McCoy, A. J., Moriarty, N. W., Oeffner, R., Read, R. J., Richardson, D. C., Richardson, J. S., Terwilliger, T. C., and Zwart, P. H. (2010) PHENIX. A comprehensive Python-based system for macromolecular structure solution. *Acta Crystallogr. D Biol. Crystallogr.* **66,** 213–221
33. McCoy, A. J., Grosse-Kunstleve, R. W., Adams, P. D., Winn, M. D., Storoni, L. C., Read, R. J. (2007) Phaser crystallographic software. *J. Appl. Crystallogr.* **40,** 658–674
34. Emsley, P., and Cowtan, K. (2004) Coot. Model-building tools for molecular graphics. *Acta Crystallogr. D Biol. Crystallogr.* **60,** 2126–2132
35. Collaborative Computational Project, Number 4 (1994) The CCP4 Suite. Programs for protein crystallography. *Acta Crystallogr. D Biol. Crystallogr.* **50,** 760–763
36. Krissinel, E., and Henrick, K. (2004) Secondary-structure matching (SSM), a new tool for fast protein structure alignment in three dimensions. *Acta Crystallogr. D Biol. Crystallogr.* **60,** 2256–2268
37. Laskowski, R. A., MacArthur, M. W., Moss, D. S., and Thornton, J. M. (1993) PROCHECK. A program to check the stereochemical quality of

protein structures. *J. Appl. Crystallogr.* **26,** 283–291
38. Heinz, D. W., Ryan, M., Bullock, T. L., and Griffith, O. H. (1995) Crystal structure of the phosphatidylinositol-specific phospholipase C from *Bacillus cereus* in complex with *myo*-inositol. *EMBO J.* **14,** 3855–3863
39. Moser, J., Gerstel, B., Meyer, J. E., Chakraborty, T., Wehland, J., and Heinz, D. W. (1997) Crystal structure of the phosphatidylinositolspecific phospholipase C from the human pathogen, *Listeria monocytogenes*. *J. Mol. Biol.* **273,** 269–282
40. Wimley, W. C., and White, S. H. (1996) Experimentally determined hydrophobicity scale for proteins at membrane interfaces. *Nat. Struct. Biol.* **3,** 842–848
41. Grauffel, C., Yang, B., He, T., Roberts, M. F., Gershenson, A., and Reuter, N. (2013) Cation-π interactions as lipid-specific anchors for phosphatidylinositol-specific phospholipase-C. *J. Am. Chem. Soc.* **135,** 5740–5750

Supplemental Information: Tables S1 and S2 and Figures S1 and S2

Cheng J, Goldstein R, Gershenson A, Stec B, Roberts MF (2013)
"The cation- π box is a specific phosphatidylcholine membrane targeting motif,"

The following table compares all proteins in the PDB as of August 2012 that contain choline, phosphocholine, phosphatidylcholine lipid, or similar choline containing ligands. Included in the chart is the identity of the protein, its organism of origin, all PDBs associated with its identity and origin, as well as its state of membrane interaction and the function of the protein. Ligands are abbreviated as per PDB codes, and a list of the abbreviations follows. The binding mode of the choline ligand is also noted, with attention focused on the nature of the coordination of the quaternary amine of the choline or choline portion of the ligand. Proteins are ordered in a general sense by function, i.e. proteins that bind choline specifically, lipid transfer proteins, esterases, etc. Highlighted in bold are any proteins that bind the quaternary amine of choline with a π-cation box type arrangement: that is, the cationic quaternary amine is held between the π systems several (usually 2-4) aromatic residues.

Table SI. Proteins in the PDB that have been shown to bind choline or choline-containing ligands.

Protein (organism)	PDBID	Membrane Interaction	Function	Ligand	Binding Mode
choline binding protein F (*Streptococcus pneumoniae*)	2V04, 2V05, 2VYU, 2X8M, 2X8O, 2X8P	soluble	choline binding protein	CHO	quaternary amine held by π-cation box
choline binding domain from autolysin (*S. pneumoniae*)	1GVM, 1H8G, 1HCX	soluble	choline binding protein	CHO	quaternary amine held by π-cation box
choline binding domain of Spr1274 (*S. pneumoniae*)	3HIA	soluble	choline binding protein	CHO	quaternary amine held in π-cation box; hydroxyl held by a phosphate via an Asn and a Ser
choline binding protein (*Sinorhizobium meliloti*)	2REG	membrane bound	ABC transporter	CHO	quaternary amine held by π-cation box, Asp and Asn form polar contacts
choline acetyl-transferase (human)	2FY3	soluble	generates acetylcholine	CHO	quaternary amine held by π-cation box
OpuBC (*Bacillus subtilis*)	3R6U, 3PPQ	soluble	choline binding protein	CHO	quaternary amine held by π-cation box
acetylcholine binding protein (*Lymnaea stagnalis*)	1UV6, 2XZ5	membrane bound	acetylcholine binding protein	CCE	quaternary amine held by π-cation box
C-reactive protein (human)	1b09	soluble	phosphocholine binding protein	PC	bound via the phosphate
PDV-109 fibronectin module (bovine)	1H8P	interfacial	choline lipid binding protein	PC	quaternary amine is held by a π-cation box
IGA-Kappa MC/PC603 FAB (mouse)	2MCP	soluble	phosphocholine binding protein	PC	quaternary amine is held by a π-cation box; phosphate is coordinated by an Arg

Protein	PDBID	Membrane Interactions	Function	Ligand	Binding Mode
immune response protein (human)	1DL7	soluble	phosphocholine binding protein	NCH	quaternary amine is held by a π-cation box; polar contacts to phosphate
phosphatidylcholine transfer protein (human)	1LN1, 1LN2, 1LN3	interfacial	PC lipid transfer protein	DLP	quaternary amine is held by a π-cation box; also held by acyl chains, ligand is very tightly bound
phosphatidylinositol transfer protein (human, rat)	1UW5, 2A1L, 1T27	interfacial	PI/PC transfer protein	PC, PCW	acyl chains and phosphate bound; choline group is apparently uncoordinated
Sec14 homolog (yeast)	3B7Q, 3B7Z	soluble	PI/PC transfer protein	6PL	quaternary amine held by π-cation box; lipid chains also bound
autolysisn (*S. pneumoniae*)	2WW5, 2WWC, 2WWD	soluble	peptidoglycanase	CHO	quaternary amine held by π-cation box
Endolysin (phage CP-1)	1OBA	soluble	peptidoglycanase	CHO	quaternary amine held by π-cation box
butyryl cholinesterase (human)	1P0M	soluble	esterase	CHO	quaternary amine held by π-cation box
phosphocholine esterase domain from CPBE (*S. pneumoniae)*	1WRA, 2BIB	interfacial	esterase	PC	mostly bound through phosphate; single π-cation interaction with quaternary amine
Acetylcholinesterase (mouse)	2HA2, 2HA3,2HA6, 2HA5, 2HA7	soluble	esterase	SCU, CHO, SCK, BCH	quaternary amine held by π-cation box, additional polar contacts bind molecule
butyrylcholine esterase (human)	1P0P	soluble	esterase	BCH	quaternary amine held by π-cation box, as well as various polar contacts on the rest of the molecule
Acetylcholinesterase (*Torpedo californica)*	2C58, 2C4H	soluble	esterase	BCH	quaternary amine held by π-cation box
choline kinase (*Plasmodium knowlesi*)	3C5I	soluble	kinase	CHO	quaternary amine held in π-cation box, hydroxide coordinated by an Asp and Glu
choline kinase α2 (human)	2CKQ	soluble	kinase	PC	quaternary amine held in π-cation box; phosphate coordinated by Ser, Asp, Asn
potassium channel (*Burkholderia psedomallei*)	2WLL	membrane bound	ion channel	PLC	bound via the phosphate only
potassium channel *(Magnetospirillum magnetotacticum*)	2x6a, 2x6b, 2x6c	membrane bound	ion channel	PC	binding to phosphate dominant; a single π-cation interaction

Protein	PDBID	Membrane Interactions	Function	Ligand	Binding Mode
Na^+ coupled betaine symporter (*Corynebacterium glutamicum*)	3P03	membrane bound	transporter	CHO	quaternary amine held by π-cation box, additional polar contacts bind molecule
LeuT (*Aquifex aeolicus*)	3USG, 3USL, 3USM,	membrane bound	sodium symporter	PC	bound by the lipid chains; no interaction with phosphocholine
ligand gated ion channel (*Aquifex aeolicus*)	3p4w, 3p50, 3uu5, 3uu8,3uub, 3EAM	membrane bound	ion channel	PLC, GPC	lipid chains are bound; polar contacts to the phosphate and glycerol; no interactions with choline
Xanthorhodopsin (*Salinibacter ruber*)	3DDL	membrane bound	ion channel	PX4	bound by the lipid chains; phosphate is visible but not bound; choline head group is not ordered
NavAB (*Arcobacter butzleri*)	3RVY, 3RVZ, 3RW0	membrane bound	voltage gated ion channel	PX4	bound by the lipid chains; phosphate is visible but not bound; choline head group is not ordered
SR calcium pump (*Oryctolagus cuniculus)*	2ZBD, 3AR2	membrane bound	ion pump	GPC	bound by lipid chains and phosphate; choline is not bound
sodium potassium pump (porcine)	3B8E	membrane bound	ion pump	GPC	bound by phosphate only; lipid chains are not ordered
voltage dependent ion anion channel (mouse)	3EMN	membrane bound	ion channel	MC3	bound by acyl chain and polar contact to glycerol; choline is not ordered
Lipase (*Thermomyces lanuginose*)	1EIN	interfacial	lipase	PLC	bound by the lipid chains only; choline is not bound
lipase-procolipase (human)	1LPA	interfacial	lipase	PLC	bound by the lipid chains only; choline is not bound
phospholipase A_2 (porcine)	1L8S	interfacial	lipase	LPE	bound by the lipid chains only; choline is not bound
Phospholipase (*Bacillus cereus*)	1P6D, 1P6E	interfacial	phospholipase	3PC, PC5	extensive coordination to sulfur (PC5); Glu coordination to the choline
cytochrome BC1 (chicken)	3H1I, 3H1J	membrane bound	mitochondrial electron transport	PLC	ligand is held by acyl chains, with 1 Asp near choline
photosynthetic reaction center (*Rhodobacter sphaeroides* R26)	2HG9,2HH1,2HG3, 2J8C, 1M3X	membrane bound	photosynthetic reaction center	PCK, GPC	held by lipid chains only
mitochondiral ADP/ATP carrier (bovine)	1OKC	membrane bound	ATP transport	GPC	coordinated by phosphate only
cytochrome BC1 complex (yeast)	1KB9	membrane bound	electron transport chain	PCF	held by lipid chain, phosphate makes polar contacts

Protein	PDBID	Membrane Interactions	Function	Ligand	Binding Mode
cytochrome BC1 complex (yeast)	1P84	membrane bound	electron transport chain	GPC	held by lipid chains only
cytochrome C oxidase (bovine)	1V54, 2DYR, 3AG2, 3AG3, 1V55, 2EIJ, 3ABM, 2ABK, 3AG4, 2EIK, 2EIL, 3ABL, 2DYS, 3AG1, 2ZXW, 2EIM, 2EIN	membrane bound	electron transport chain	PSC	held by choline head group with 1 Tyr, and 1 Asp, extensive polar contacts with phosphate, complete hydrophobic interaction with the acyl chain
cytochrome BC1 complex (yeast)	1P84	membrane bound	electron transport chain	GPC	held by lipid chains only
cytochrome C oxidase (*Paracoccus denitrificans*)	1QLE	membrane bound	electron transport chain	GPC	held by lipid chains and polar contact to phosphate
cytochrome B6F (*Nostoc* sp. PCC7120*)*	2ZT9	membrane bound	electron transport chain	OPC	held by lipid chain; phosphate makes polar contacts
ATP synthase rotor ring (*Bacillus pseudofirmus*)	2X2V	membrane bound	ATP synthesis	DPV	bound by lipid chain and phosphate polar contacts; Glu coordinates quaternary amine
cytochrome B6F (*Mastigocladus laminosus*)	2E74, 2E75, 2E76, 1Vf5, 2D2C	membrane bound	electron transport chain	OPC	bound by lipid chains only; PC head group is far above the protein surface
nuclear liver receptor homolog (human)	4DOS	soluble	binds phospholipids	PLC	lipid chains and phosphate are bound; choline group sticks out above protein surface
Lipovitellin (*Ichtyomyzon unicuspis*)	1LSH	interfacial	lipid and metal storage	PLC	bound by lipid chains only; PC head group is far above the protein surface
bacteriacidal/perme-ability increasing protein (human)	1EWF, 1BO1	interfacial	Lipopolysaccha-ride binding	GPC	lipid chains and phosphate are bound; choline sticks out above the surface of the protein
non-specific lipid transfer protein (wheat)	1BWO, 1MID	membrane bound	lipid transfer protein	LPC	bound by lipid chain; phosphate and glycerol make polar contacts; choline is above the surface of the protein
GM2-activating protein (human)	2AG2	interfacial	lysosomal lipid transfer protein	LP3	bound by lipid chains only
SF-1 (mouse)	3F7D	interfacial	lipid binding nuclear receptor	P42	lipid chains and phosphate are bound; choline group sticks out above protein surface
Wnt inhibitory factor 1 (human)	2YGN, 2YGO, 2YGP, 2YGQ	soluble	growth factor inhibitor	PCF	single Phe within π-cation distance; but mostly held by lipid chains

Protein	PDBID	Membrane Interactions	Function	Ligand	Binding Mode
Wnt inhibitory factor 1 (human)	2YGN, 2YGO, 2YGP, 2YGQ	soluble	growth factor inhibitor	PCF	single Phe within π-cation distance; but mostly held by lipid chains
calmodulin (bovine)	3IF7	soluble	Ca^{2+} binding protein	SPU	lipid chains bound; choline is coordinated by two Glu
Rhodopsin (squid)	2Z73	membrane bound	GPCR	GPC	bound by lipid chain; phosphate and glycerol make polar contacts; choline not ordered
rhomboid protease GLPG (*E. coli*)	2XTV	membrane bound	protease	MC3	lipid chains bound; polar contact with phosphates; cholines are above the surface of the protein
SNARE ykt6 longin domain (rat)	3KYQ	interfacial	membrane fusion protein	DPV	bound by lipid chains, polar contacts, and a single π-cation interaction with quaternary amine
pore-forming cytolysin sticholysin II (*Stichodactyla helianthus*)	1O72	interfacial	pore forming protein	PC	quaternary amine held by π-cation box
leukociden F (*Staphylococcus aureus*)	3LKF	interfacial	self assembling channel forming protein	PC	quaternary amine held by a π-cation; phosphate bound by Arg
lens specific aquaporin (*Ovis aries*)	2B6O	membrane bound	water pore forming protein	MC3	bound by lipid chain; phosphate makes polar contacts; choline is above the surface of the protein
bacterial dynamin-like protein (*Nostoc punctiforme*)	2W6D	membrane bound	membrane fusion protein	CPL	held by phosphates or lipid chains, not choline
GM2 activator protein (human)	1TJJ	soluble	lipid transfer protein	PFS	lipid chains are bound; polar contacts are formed with the phosphates
phosphoethanolamine methyltranserase (*Plasmodium falciparum*)	3UJ9, 3UJC, 3UJD	soluble	methyl transferase	PC	mostly coordinated by the phosphate; one π-cation interaction with quaternary amine
CD1D antigen (mouse)	2FIK, 2GAZ, 2H26, 1ZHN	soluble	lipid binding antigen protein	6PL, PC6	acyl chains only; PC head group is far above the protein surface
MD-1 lymphocyte antigen (mouse)	3M7O	soluble	antigen	L9R	ligand bound via lipid chains and polar contacts with phosphate; one π-cation interaction with the amine
CD1b3 (bovine)	3L9R	soluble	antigen?	L9R	bound via acyl chains; phosphocholine is above the surface of the protein

Protein	PDBID	Membrane Interactions	Function	Ligand	Binding Mode
L-ficolin (human)	2J0H	soluble	lectin-like immune defense protein	ACH	anchored via acetyl group
BmrR (*B. subtilis*)	3Q5S	soluble	multidrug resistance gene	ACH	anchored via acetyl group
PaCTD (*Pseudomonas arvilla*)	2AZQ, 1DMH, 1DLT, 1DLM, 1DLQ	interfacial	1,2 dioxygenase	PCF	bound via lipid chains and glycerol group; phosphocholine sticks up above the protein
hydoxyquinol 1,2 dioxygenase (*Nocardioides simplex*)	1TMX, 3N9T, 1S9A	soluble	dioxygenase	HGX	bound via acyl chains; phosphocholine is not ordered
Rho 1,2-CTD (*Rhodococcus opacus*)	3HHY,3HJS, 3I51, 3HKP, 3I4Y, 3HGI, 3HHX,3HJQ, 3I4V, 3HJ8	soluble	dioxygenase	6PL	bound by lipid chain and polar contacts to the glycerol

Ligand abbreviations in Table SI.

Abbreviation	compound
3PC	(3S)-3,4-di-N-hexanoyloxybutyl-1-phosphocholine
6PL	1-palmitoyl-2-stearoyl-sn-glycero-3-phosphocholine
ACH	acetylcholine
BCH	butyrylthiocholine
CCE	carbamylcholine
CHO	choline
CPL	1-palmitoyl-2-linoleoyl-phosphatidylcholine
DLP	1,2-dilinoleoyl-sn-glycero-3-phosphocholine
DPV	n-dodecylphosphocholine
GPC	glycerophosphocholine
HGX	1-heptadecanoyl-2-tridecanoyl-3-glycerolphosphonylcholine
L9R	1-stearoyl-2-oleoyl-sn-glycero-3-phosphocholine
LP3	(7R)-4,7-dihydroxy-N,N,N-trimethyl-10-oxo-3,5,9-trioxa-4-phosphaheptacosan-1-aminium 4-oxide
LPC	(1-myristoyl-glycerol-3-yl)phosphonylcholine
LPE	1-O-octadecyl-sn-glycerol-3-phosphocholine
MC3	1,2-dimyristoyl-rac-glycerol-3-phosphocholine
NCH	p-nitrophenylphosphocholine
OPC	dioleoylphosphatidylcholine
P42	1-stearoyl-2-palmitoyl-sn-glycero-3-phosphocholine
PC	phosphocholine
PC5	1,2-di-N-pentanoyl-sn-glycero-3-dithiophosphocholine
PC6	7-[(dodecanoyloxy)methyl]-4-hydroxyl-N,N,N-trimethyl-9-oxo-3,5,8-trioxa- 4-phosphado-triacontan-1-aminium 4-oxide
PCF	1,2-dipalmitoylphosphatidylcholine
PCK	1,2-distearoyl(9,10-dibromo)-sn-glycero-3-phosphocholine
PCW	1,2-dioleoyl-sn-glycero-3-phosphocholine
PFS	1-O-octadecyl-2-acetyl-sn-glycerol-3-phosphocholine
PLC	diundecylphosphatidylcholine
PSC	1-palmitoyl-2-linoleoyl-sn-glycerol-3-phosphocholine
PX4	1,2-dimyristoyl-sn-glycero-3-phosphocholine
SCK	succinyl dicholine
SCU	succinylcholine

Table S1 shows one overwhelming theme: if a protein specifically binds choline, either as the substrate or product of a reaction, or as a moiety to be transferred, it does so via a protein π-choline cation box. Proteins that bind lipids and are non-specific as to the head group, or proteins which are integral membrane proteins, bind ligand mostly via the lipid chains, or possibly via interactions with the phosphate. Out of 12 proteins that have choline as a ligand, all 12 bound choline via a π-cation box. Similarly, of the 10 proteins that contain phosphocholine, 9 bound the quaternary amine in a π-cation box, while one did not. Conversely, of the 41 proteins that bound phospholipids with a choline head group, only a few had π-cation interactions, and of these there was usually only a single defined interaction of the cation with an aromatic group. Overall, of the 67 different proteins that bind choline or choline containing ligands, 43% of them bind the choline via a π-cation interaction.

HEPES binding to N254Y/H258Y

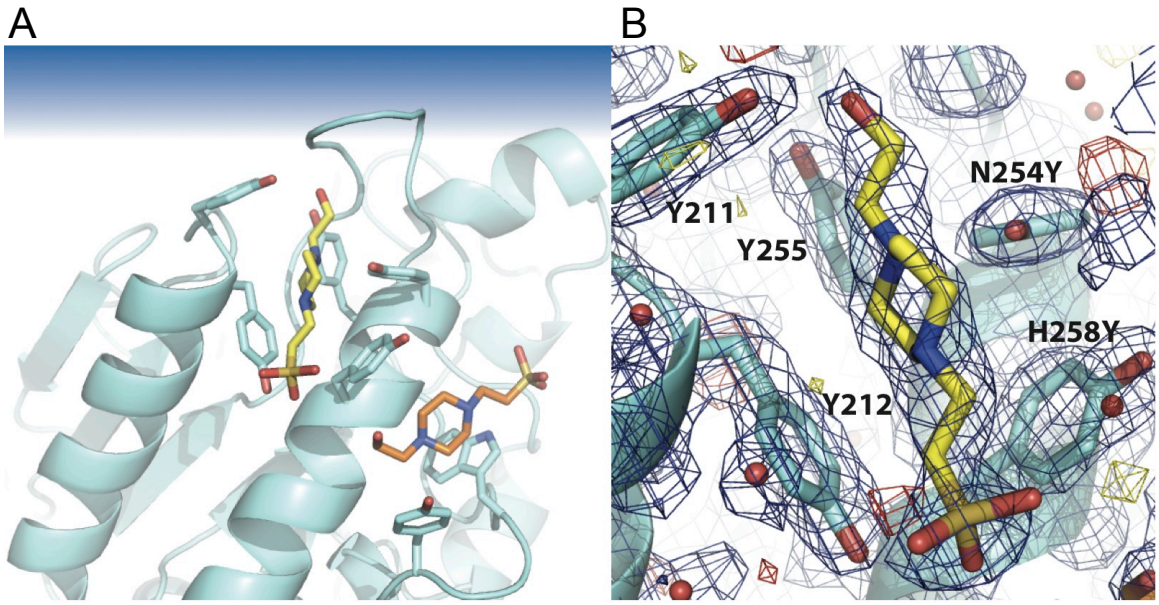

Figure S1. (A) N254Y/H254Y structure with HEPES in the choline binding site (PDB 4F2Y). Representative electron density for HEPES ligands (B). Electron density shown in dark blue and contoured at 1σ, is shown with the model superimposed.

Initially, we generated crystals of N254Y/H258Y from a solution containing 10% isopropanol, 22% PEG 4000, and 100 mM HEPES, pH 7.5. Prior to crystallization, the protein was incubated with 30 mM glycerophosphocholine and 1 mM diC_7PC for 2 h, though neither of these molecules was evident in the structure. Instead two molecules of HEPES were observed in the helix F/G region (Figure S2). In contrast, when wild type *S. aureus* PI-PLC was crystallized under similar conditions, no small molecules were bound in this region. In this N254Y/H258Y structure (PDB entry 4I9M) one HEPES molecule lies in choline binding site 1, directly between helices F and G, with a cationic nitrogen held between the π systems of Tyr212 and Tyr258. Likewise the cationic nitrogen of the second molecule of HEPES is held in choline binding site 2, between the π systems of Trp287, Tyr290 and Tyr258. Tyr254 provides edge face interactions with Tyr258. In order to accommodate the HEPES molecule in the binding pockets, the side chain of Tyr212 must rotate downward from its position in the unliganded double mutant structure by 94°, while the side chain of Tyr258 must rotate upward 99°. The rotation of Tyr212 forms the left sidewall of binding site one, while Tyr258 forms the right side of this binding site, as well as the left side of binding site two.

Previously, we obtained a structure of H258Y crystallized in acidic conditions (Goldstein et al (2012) *Biochemistry* 51: 2579-2587), but more recently obtained crystals of this mutant protein from a solution containing 10% isopropanol, 22% PEG 4000, and 100 mM HEPES, pH 7.5. The basic H258Y structure (PDB entry 4I9T) has no clear indication of HEPES occupying the sites seen in N254Y/H258Y, although there was some electron density consistent with a low occupancy (<30%) ligand bound in site 2. However, the refinement is best with a small PEG molecule at that site. The reason for the decreased affinity for HEPES in the H258Y single mutant becomes clear when examining the side chains of the binding pockets. Without the mutation N254Y, the edge face interaction between Tyr254 and Tyr258 is lost, this allows the side chain of Tyr258 to exist in either the two distinct positions – one without a ligand (57%) or one where a ligand is present (43%). More importantly, without the mutation of Asn254 to the significantly larger Tyr residue, the side chain of Tyr212 is not completely rotated down into the mutant conformation, and instead appears primarily in the conformation of the WT structure (70%) rather than that of the HEPES bound mutant structure (30%). This implies that both N254Y and H258Y are needed for discrete PC binding to the *S. aureus* PI-PLC.

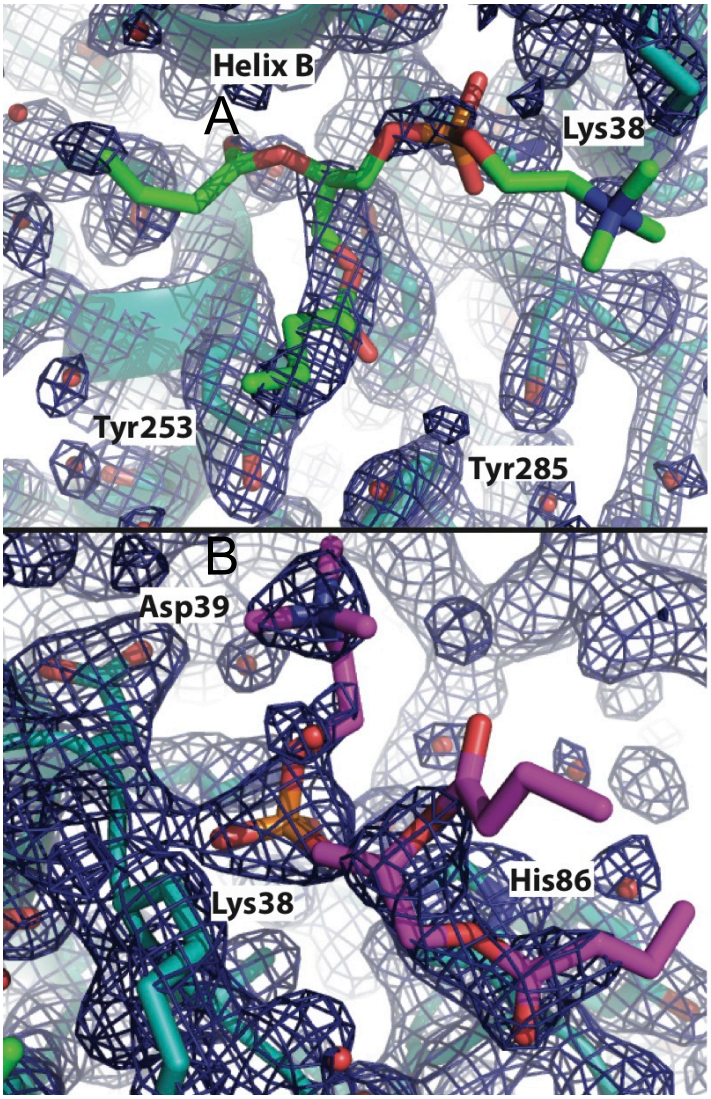

Figure S2. View of the two auxiliary diC_4PC molecules found in the N254Y/H258Y crystal.

(A) One phospholipid, under helix B, is bound most likely by hydrophobic interactions of one acyl chain with Tyr253 and Tyr585, although the overall the density is mediocre.

(B) The secondary auxiliary phospholipid is bound in the anion binding site described in the WT protein (Cheng et al. (2012) *J. Biol. Chem.* 287, 40317-40327). The phosphate is coordinated by Lys38 and His86; densities for the phosphate, quaternary amine, and glycerol backbone are excellent, while the lipid chains are more mobile. Electron density, shown in dark blue in both, is for 2Fo-Fc at 1 σ.

Table S2. Crystallographic data for selected *S. aureus* PI-PLC crystals.

Crystal	N254Y/H258Y + HEPES	H258Y: Basic
PDB ID	4I9M	4I9T
Resolution Range (Å)	2.19-30.85	1.99-37.63
No. of reflections	15898	20933
Reflections in free set	795	1072
Space group	$P2_12_12_1$	$P2_12_12_1$
Unit cell		
a (Å)	86.22	85.59
b (Å)	56.12	57.83
c (Å)	61.71	60.78
Completeness	99.5%	99.3%
R_{merge}	11.7	7.6
Protein molecules in A.U.	1	1
R_{cryst} [a]	0.1580	0.1786
R_{free} [b]	0.2358	0.2324
No. residues	304	305
No. non-hydrogen protein atoms	2437	2498
No. H_2O molecules	342	195
No. SO_4^{-2} ions	1	1
r.m.s.d. bonds (Å)	0.02	0.20
r.m.s.d. angles (^{o})	1.70	1.98
Ramachandran plot (%)		
Most favored	90.1	96.49
Additionally allowed	9.9	3.19
Generously allowed	0	0.32
Disallowed	0	0
Average B-factor (Å^2)	33.45	25.64

[a] $R_{cryst} = \{\Sigma\ (||F_o| - |F_c||) / |F_o|\}$, where $|F_o|$ and $|F_c|$ are the observed and calculated structure factor amplitudes, respectively.

[b] Brunger (1992).

The Cation-π Box Is a Specific Phosphatidylcholine Membrane Targeting Motif

Jiongjia Cheng, Rebecca Goldstein, Anne Gershenson, Boguslaw Stec and Mary F. Roberts

J. Biol. Chem. 2013, 288:14863-14873.
doi: 10.1074/jbc.M113.466532 originally published online April 10, 2013
